Organic & Biomolecular Chemistry

PAPER

View Article Online
View Journal

Dynamic self-inclusion behavior of pillar[5]arene-based pseudo[1]rotaxanes†

Cite this: DOI: 10.1039/c3ob42044b

Yangfan Guan,[a] Pingying Liu,[b] Chao Deng,[a] Mengfei Ni,[a] Shuhan Xiong,[a] Chen Lin,[a] Xiao-Yu Hu,*[a] Jing Ma*[b] and Leyong Wang*[a]

Received 12th October 2013,
Accepted 18th November 2013

DOI: 10.1039/c3ob42044b

www.rsc.org/obc

It was found that spontaneous isomerization takes place between three isomers of a pillar[5]arene (**P5**)-based pseudo[1]rotaxane. The isomerization process could be monitored by ^{1}H NMR spectra in polar solvent and the geometric configurations of the three isomers were further evaluated by theoretical calculations. In the threaded forms, the alkyl side chain might be preorganized by intramolecular N–H···O bonds between the urea group of the side chain and the methoxy group of the **P5** and further stabilized by multiple interactions, including H-bonding, C–H···π interactions, and the steric effect of the *N*-Boc moiety. These cooperative interactions greatly enhance the stability of the threaded form in polar solvent, and endow it with very special self-inclusion behavior.

Introduction

Among various interlocked architectures,[1] pseudo[1]rotaxane is a special type of supramolecular system that contains both the wheel and axle in one molecule, with a fast or slow exchange process between threaded and open forms. The threaded structure of pseudo[1]rotaxane has been successfully proved by many researchers *via* spectroscopic measurements,[2] solid structure analysis[3] or the introduction of a stopper unit to form the [1]rotaxane.[4] In particular, pseudo[1]rotaxanes and [1]rotaxanes can be extensively used as molecular machines to show corresponding responses to some specific stimuli due to their reversible conversion behavior, and many functionalized macrocyclic molecules have been synthesized for this purpose.[4b,5]

Ever since the discovery of pillararene,[6] pillar[5]arenes (**P5**) continue to be attractive wheel components in constructing interlocked assemblies, and various pillararene-based pseudorotaxanes with diverse functions have been reported in the last few years.[7] For example, Cao and co-workers[8] reported that pillar[5]arene-based pseudorotaxanes selectively bound dihalogen alkanes in non-polar solvent. Hou *et al.*[9] reported that the amide group was introduced to the side-chain of **P5** to tune the resulting axle toward the inner space of the **P5** cavity by intramolecular H-bonding, leading to the formation of a pseudo[1]rotaxane structure, which will accelerate the aminolysis by enhancing the stability of the intermediate. Ogoshi's work[10] had shown that an octyltrimethyl ammonium functionalized **P5** predominantly formed a self-inclusion complex structure in $CHCl_3$. However, previously reported pseudo[1]-rotaxanes shared the following characteristics: (1) it is difficult or impossible to separate the open and threaded forms of a pseudo[1]rotaxane due to their dynamic behavior; (2) especially, a highly polar solvent would prevent H-bond or C–H···π interactions between the alkyl chain and **P5** cavity. Thus pillararene-based pseudorotaxanes in polar solvent have been the subject of only a few reports.[7a,11] (3) In general, the large stoppers in the axle keep the axle from being included into the **P5** cavity due to their steric effect.

On the basis of our previous study of the pseudo[2]rotaxanes assembled by urea-modified pillar[5]arene and linear guests,[11,12] we describe here the preparation of an unconventional pseudo[1]rotaxane, whose pure open and threaded forms could be isolated by column chromatography temporarily. In particular, the pure open and threaded forms could both spontaneously and slowly isomerize into the other as well as the third isomer in polar solvent (DMSO) and reached equilibrium after four months at 20 °C. Moreover, the influence of the stopper size and urea moiety on the self-inclusion behavior of pseudo[1]rotaxanes in our case was discussed in detail, where, especially, the size of the *N*-Boc stopper cooperating with other non-covalent interactions could enhance the stability of the self-inclusion structure, instead of preventing the self-inclusion of the axle. In addition, the formation pathway of this pseudo[1]rotaxane is also proposed and supported by control experiments.

[a]*Key Laboratory of Mesoscopic Chemistry of MOE, Center for Multimolecular Chemistry, School of Chemistry and Chemical Engineering, Nanjing University, Nanjing 210093, China. E-mail: huxy@nju.edu.cn, lywang@nju.edu.cn*
[b]*Institute of Theoretical and Computational Chemistry, Nanjing University, Nanjing 210093, China. E-mail: majing@nju.edu.cn*

† Electronic supplementary information (ESI) available: ^{1}H and ^{13}C NMR spectra and theoretical calculation data. See DOI: 10.1039/c3ob42044b

Results and discussion

Synthesis, isolation, and structural characterization of 1_{conf1}/1u

According to the literature method,[13] amino-functionalized pillar[5]arene **8** was reacted with the di-substituted amine **9** in chloroform at 25 °C for 24 h, and then one major product **1u** together with a small fraction of the minor product $\mathbf{1}_{conf1}$ were observed as two independent spots on TLC, and then the pure **1u** and $\mathbf{1}_{conf1}$ were obtained by column chromatography, respectively (yields of 56% for **1u**, 6% for $\mathbf{1}_{conf1}$) (Fig. 1A), where the major product **1u** was expected to be a non-inclusion complex and the minor product $\mathbf{1}_{conf1}$ could be an unexpected inclusion complex.

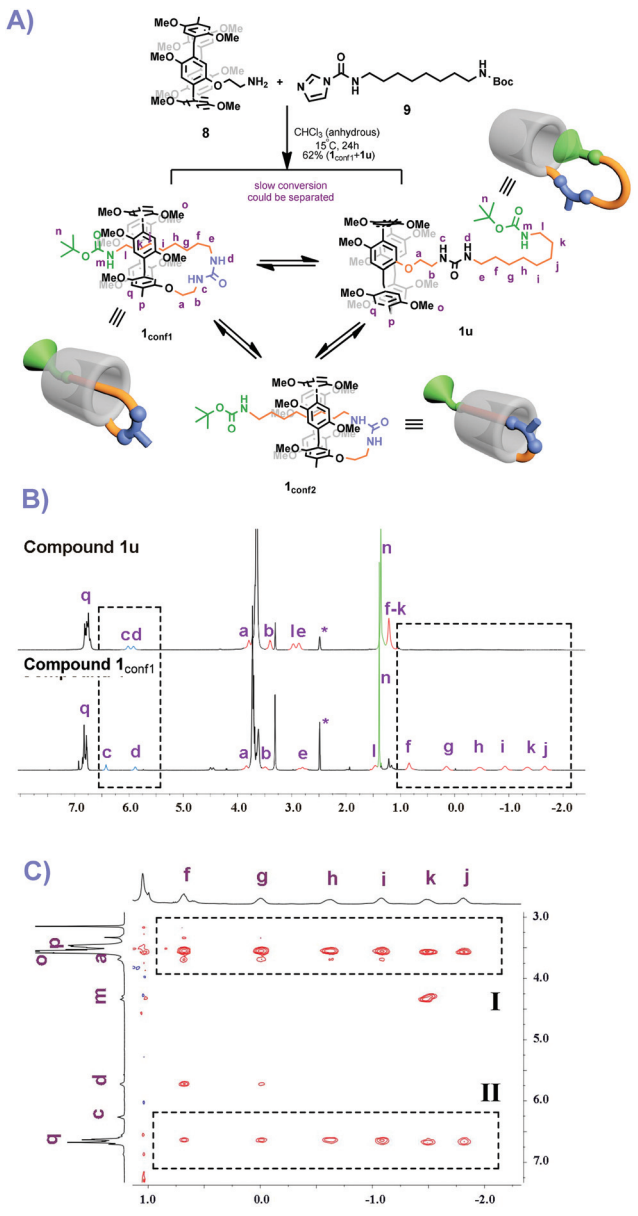

Fig. 1 (A) Schematic representation of the synthesis of $\mathbf{1}_{conf1}$ and **1u**; (B) ^{1}H NMR spectrum of $\mathbf{1}_{conf1}$ and **1u** (400 MHz, DMSO-d_6, 298 K), the peaks marked with * are ascribed to DMSO-d_6; (C) Partial 2D ROESY spectrum of $\mathbf{1}_{conf1}$ (400 MHz, DMSO-d_6, 298 K).

Initially, the structural characterization of the pure major product **1u** and minor product $\mathbf{1}_{conf1}$ was investigated by NMR spectroscopy. After four days, ^{1}H NMR spectra of both products became complicated with new peaks appearing compared to the freshly purified ones. Hence, in order to achieve their pure spectra, NMR experiments were carried out within 6 h after the pure product was isolated by column chromatography, and full characterization of **1u** and $\mathbf{1}_{conf1}$ by NMR spectroscopy was accomplished always with freshly purified products. Since the urea protons of **1u** and $\mathbf{1}_{conf1}$ both disappeared in their ^{1}H NMR spectra in $CDCl_3$ and their alkyl chain signals became broad as well, all their characterizations were then carried out in DMSO-d_6. Based on their ^{1}H NMR spectra, the major product **1u** differs from the minor product $\mathbf{1}_{conf1}$ mainly in two regions (Fig. 1B): (1) the two urea proton peaks of **1u** are adjacent (6.02 and 5.92 ppm); but in the spectrum of $\mathbf{1}_{conf1}$, H_c shifts downfield to 6.4 ppm, while the other one H_d is located at 5.90 ppm, suggesting that H_c of the ureido might be involved in stronger H-bonding interactions than H_d. (2) In the spectrum of **1u**, no peak can be obviously observed in the range of 0.5 to −2.0 ppm, suggesting the side chain of **1u** deviates from the macrocycle cavity, which confirmed that **1u** was a non-inclusion complex as expected. In the spectrum of $\mathbf{1}_{conf1}$, the four peaks corresponding to the four methylene protons H_h, H_i, H_k and H_j (−0.43, −0.91, −1.33, and −1.65 ppm) were remarkably observed in the high field, whereas H_e and H_f of the alkyl side chain were observed with a slight upfield shift compared to **1u**. These results indicated that the four methylene protons H_h, H_i, H_k and H_j in $\mathbf{1}_{conf1}$ were located in the central position of the **P5** cavity to achieve an inclusion complex, and H_e of the methylene connecting to urea moiety stayed outside the **P5** cavity.

The above ^{1}H NMR spectra undoubtedly reveal the inclusion structure of $\mathbf{1}_{conf1}$. However, is this inclusion structure a self-inclusion or interpenetration structure? In other words, does $\mathbf{1}_{conf1}$ exist as a pseudo[1]rotaxane structure, dimers, trimers, or *n*-mers in polar solvent? In order to resolve this structural question, we first measured the ^{1}H NMR spectra of $\mathbf{1}_{conf1}$ at different concentrations in the range of 1.0–60 mM (Fig. S2†), which showed that the ^{1}H NMR spectra of $\mathbf{1}_{conf1}$ is concentration independent, suggesting that $\mathbf{1}_{conf1}$ exists predominantly in the form of the pseudo[1]rotaxane or cyclic oligomer in polar solvent. Subsequently, high resolution electrospray ionization mass spectrometry (HR-ESI-MS) investigation was performed, in which two indicative peaks corresponding to $[M + H]^+$ at *m*/*z* 1050.5686 and $[M + Na]^+$ at *m*/*z* 1072.5504 were clearly observed and no other peaks corresponding to higher molecular weight interlocked structures were observed, confirming the presence of $\mathbf{1}_{conf1}$ as the pseudo[1]rotaxane structure. The 2D ROESY spectrum of $\mathbf{1}_{conf1}$ exhibits clear NOE correlations between protons H_f, H_g, H_h, H_i, H_j, H_k of the aliphatic chain and the methoxy protons H_o (Fig. 1C, cross-peaks I) and the aromatic protons H_q of **P5** (Fig. 1C, cross-peaks II), also supporting the formation of the self-inclusion structure of $\mathbf{1}_{conf1}$. Furthermore, the ROESY spectrum of $\mathbf{1}_{conf1}$ displayed very clear NOE correlations

between protons H_c and H_d of the urea group and protons H_o of the methoxy moiety, respectively, as well as between protons H_m of the amide group of *N*-Boc and protons H_o of the methoxy moiety (Fig. S3,† cross-peaks III). These correlations indicated that $\mathbf{1}_{conf1}$ was possibly stabilized by two types of N–H···O bonds, one between the *N*-Boc moiety and the methoxy group of **P5**, and the other between the urea group and the methoxy group of **P5**.

Transformations between $\mathbf{1}_{conf1}$, $\mathbf{1}_{conf2}$ and 1u

As mentioned above, we found that pure $\mathbf{1}_{conf1}$ or **1u** gradually turned into mixtures of isomers in DMSO after days, where, interestingly, the third isomer $\mathbf{1}_{conf2}$ could be observed but could not be isolated by column chromatography. Initially, time-dependent ^{1}H NMR of sample $\mathbf{1}_{conf1}$ was performed to investigate the transformation of pure $\mathbf{1}_{conf1}$ to **1u** and the third isomer $\mathbf{1}_{conf2}$ (Fig. 2A–2D) in DMSO-d_6 at 20 °C. We found that after 77 h (Fig. 2B), two new peaks at 6.15 and 6.00 ppm (colored in purple) corresponding to the urea protons H_c and H_d of **1u** (colored in purple) appeared and the peak intensity of $\mathbf{1}_{conf1}$ (colored in red) decreased to 91% of its initial value (based on the peak integration of H_g). Moreover, another set of peaks (0.51, −0.07, −0.81, −1.82, −1.95 ppm, colored in green) that we assigned to the third isomer $\mathbf{1}_{conf2}$ emerged, which could be another conformation of a self-inclusion structure different from $\mathbf{1}_{conf1}$. After 289 h (Fig. 2C), the newly appeared urea protons H_c and H_d of **1u** became broad and the peak intensity of $\mathbf{1}_{conf1}$ decreased to 30% of its initial value in the spectra, where the molar ratio of **1u**/$\mathbf{1}_{conf1}$/$\mathbf{1}_{conf2}$ was calculated by the peak integration to be 55/30/15. After 4 months, the peak intensity of H_g of $\mathbf{1}_{conf1}$ still kept 24% of its initial value (Fig. 2D) in the spectra, where the molar ratio of **1u**/$\mathbf{1}_{conf1}$/$\mathbf{1}_{conf2}$ was then calculated to be 60/24/16, implying that the system of the self-inclusion structures $\mathbf{1}_{conf1}$, $\mathbf{1}_{conf2}$ and the non-inclusion structure **1u** reached equilibrium at 20 °C in DMSO-d_6, where the open structure **1u** and self-inclusion structure $\mathbf{1}_{conf2}$ were both transformed from self-inclusion structure $\mathbf{1}_{conf1}$.

Subsequently, the transformation from pure non-inclusion structure **1u** into $\mathbf{1}_{conf1}$ and $\mathbf{1}_{conf2}$ was able to be similarly observed from the time-dependent ^{1}H NMR spectra of pure non-inclusion structure **1u** in DMSO-d_6 at 20 °C (Fig. 2E–2H). The pure non-inclusion compound **1u** showed no signal in the high field of ^{1}H NMR spectra, but after 141 h, two new and independent sets of signals in the high field of ^{1}H NMR spectra corresponding to $\mathbf{1}_{conf1}$ and $\mathbf{1}_{conf2}$ were observed with the peak integration ratio of 1 : 25 (Fig. 2F, colored in red and green, respectively), which then changed into 1 : 4 after 261 h.

We have deduced the formation of two types of hydrogen bonds between the urea/amide group and the methoxy group in $\mathbf{1}_{conf1}$, and it is well known that the fluoride ion shows a strong binding ability to N–H bonds even in polar solvents,[14] therefore, we added fluoride ions into the solution of $\mathbf{1}_{conf1}$ to investigate the effect of fluoride ions in our system. At the beginning, the spectrum of pure $\mathbf{1}_{conf1}$ showed only one set of peaks for H_{g-j} in the high field (Fig. 3A, colored in red). After 165 h, the peaks assigned to $\mathbf{1}_{conf2}$ (Fig. 3B, colored in green) and **1u** (Fig. 3B, colored in purple) were observed, indicating $\mathbf{1}_{conf1}$ partially transformed into $\mathbf{1}_{conf2}$ and **1u** as mentioned above. Then an excess amount of tetra-*n*-butylammonium fluoride salt was added into the NMR tube, and the resulting spectrum is shown in Fig. 3C: in the low field, the urea proton H_d and the amide proton H_m of $\mathbf{1}_{conf1}$ together with the urea proton H_d of **1u** shifted downfield to ~7.7, 6.4, 8.2 ppm and became broad, while the urea proton H_c of $\mathbf{1}_{conf1}$ remained unchanged due to the stable intramolecular H-bonding, and it

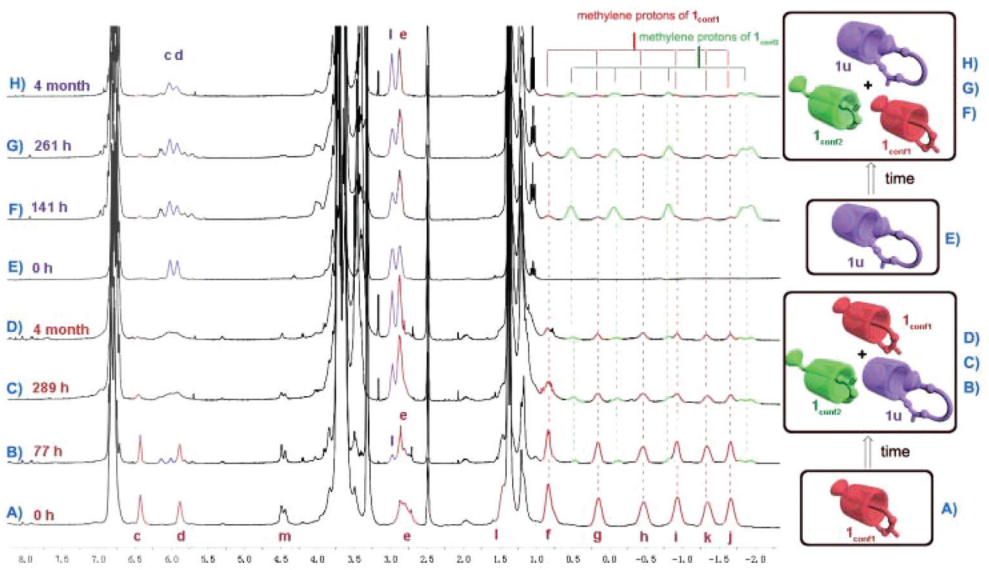

Fig. 2 Time-dependent transformation of $\mathbf{1}_{conf1}$ and **1u** monitored by ^{1}H NMR spectra (400 MHz, DMSO-d_6, 298 K). (A) compound $\mathbf{1}_{conf1}$, (B) $\mathbf{1}_{conf1}$ after 77 h, (C) $\mathbf{1}_{conf1}$ after 289 h, (D) $\mathbf{1}_{conf1}$ after 4 months, (E) compound **1u**, (F) **1u** after 141 h, (G) **1u** after 261 h, and (H) **1u** after 4 months. The color of the proton signals were in accordance with 3D cartoon models: $\mathbf{1}_{conf1}$ in red, **1u** in purple and $\mathbf{1}_{conf2}$ in green.

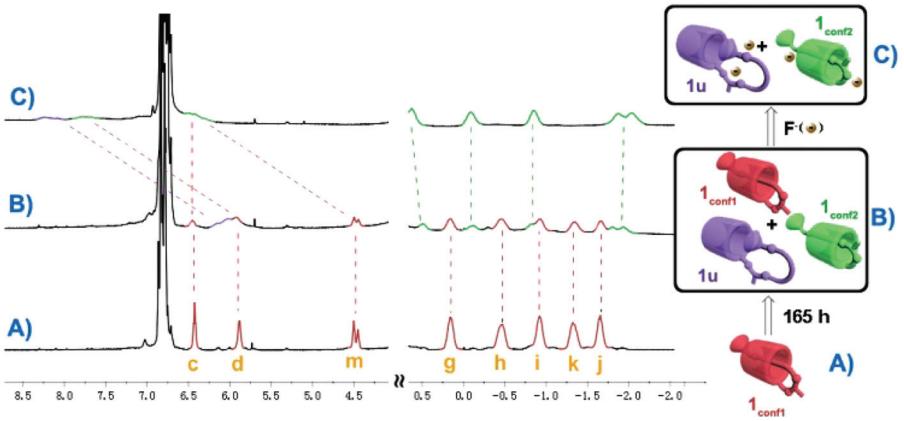

Fig. 3 Fluoride ion induced transformation from $\mathbf{1}_{conf1}$ to $\mathbf{1}_{conf2}$ monitored by ^{1}H NMR spectra (400 MHz, DMSO-d_6, 298 K). (A) Pure compound $\mathbf{1}_{conf1}$, (B) $\mathbf{1}_{conf1}$ after 165 h, and (C) upon addition of excess amount of tetra-*n*-butylammonium fluoride salt.

was overlapped with the downfield shifted proton H_m of $\mathbf{1}_{conf1}$; in the high field (from 0.5 to −2.0 ppm), the signals of $\mathbf{1}_{conf1}$ disappeared upon addition of F^- and the resulting signals were highly similar to that of $\mathbf{1}_{conf2}$. Based on these observations, it seemed that the fluoride ion functioned as an accelerator for the transformation from $\mathbf{1}_{conf1}$ to $\mathbf{1}_{conf2}$, probably because fluoride ions could strongly bind H_m of the amide group forcing the end of the axle of $\mathbf{1}_{conf1}$ to slip away from the rim of the cavity to achieve another self-inclusion isomer, $\mathbf{1}_{conf2}$, where the H-bonds between the amide group and methoxy groups of **P5** were broken by F^- but H_c of the urea group maintained its intramolecular H-bonds with the methoxy group of **P5**.

Therefore, on the basis of these experimental data, theoretical calculations for the conformations of $\mathbf{1}_{conf1}$, $\mathbf{1}_{conf2}$ and **1u** were carried out with the Gaussian 09 program package[15] to optimize the conformations of $\mathbf{1}_{conf1}$ and $\mathbf{1}_{conf2}$ (Fig. 4) and further compute the ^{1}H NMR chemical shifts and vibrational frequencies using density functional theory (DFT) with the M062X functional and the 6-31G(d,p) basis set. The theoretical calculation results supported the conformations of $\mathbf{1}_{conf1}$ and $\mathbf{1}_{conf2}$ (Fig. 4): the two N–H bonds of the urea group oriented in opposite directions in both $\mathbf{1}_{conf1}$ and $\mathbf{1}_{conf2}$ due to the intramolecular hydrogen bonds. The difference between conformation $\mathbf{1}_{conf1}$ and $\mathbf{1}_{conf2}$ was caused by the different hydrogen bonding sites between the alkyl side chain and **P5**: in $\mathbf{1}_{conf1}$, the amide group of *N*-Boc and the urea group of the alkyl side chain formed two types of H-bonds with the methoxy group of **P5**, resulting in a "loosen" style conformation; while in $\mathbf{1}_{conf2}$ the stronger hydrogen bonds between the inverted urea of the alkyl side chain and **P5** forced the alkyl side chain more deeply to thread into the cavity of **P5**, making the *N*-Boc end of the side chain stay away from the rim of **P5** with the hydrogen bonds between the alkyl side chain and **P5** no longer present. Thus the conformation of $\mathbf{1}_{conf2}$ could be described as a "contract" style. Probably, the tension of the urea group in $\mathbf{1}_{conf1}$ is the driving force for the transformation of $\mathbf{1}_{conf1}$ to $\mathbf{1}_{conf2}$. In addition, the results showed that $\mathbf{1}_{conf1}$ is the most stable among the three isomers $\mathbf{1}_{conf1}$, $\mathbf{1}_{conf2}$ and **1u** (Table S1†), and the energy of $\mathbf{1}_{conf2}$ is only 3.38 kcal mol^{-1} higher than $\mathbf{1}_{conf1}$, which probably could explain the reason why $\mathbf{1}_{conf1}$ and $\mathbf{1}_{conf2}$ exist as conformational isomers but $\mathbf{1}_{conf2}$ could not be separated. The calculated ^{1}H NMR chemical shifts of $\mathbf{1}_{conf1}$ are in accordance with its experimental data (Fig. S65a†), and the calculated chemical shifts of $\mathbf{1}_{conf2}$ are quite different from the experimental results of $\mathbf{1}_{conf1}$ (Fig. S65b†), supporting the different conformations between $\mathbf{1}_{conf1}$ and $\mathbf{1}_{conf2}$. Moreover, the calculated ^{1}H NMR spectrum of **1u** and IR spectrum of $\mathbf{1}_{conf1}$ are also consistent with their experimental data (Fig. S66 and S67†).

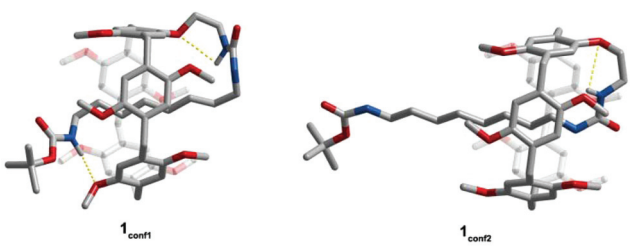

Fig. 4 The optimized geometries of the pseudo[1]rotaxane $\mathbf{1}_{conf1}$ (left) and $\mathbf{1}_{conf2}$ (right) at the M062X/6-31G(d,p) level using the PCM model (only the hydrogen atoms involved in H-bonding are shown for clarity).

Influence of the stopper size on self-inclusion behavior

For the pillar[5]arene-based AB type derivatives which contain a **P5** macrocycle and a side chain with a stopper at the end, "small" size stoppers (such as a bipyridine moiety and an alkyl chain) only formed un-interlocked pseudorotaxanes with fast rates of the alkyl chain's slipping in and out, while "large" size stoppers (such as the adamantyl group,[16] 3,5-di-*tert*-butylbenzene,[17] 3,5-dinitrobenzene,[18] and ureidopyrimidinone motif[19]) prevented the side chain from threading or dethreading. The *tert*-butoxy carbonyl group in $\mathbf{1}_{conf1}$ is a middle sized stopper, therefore, does this specific size contribute to the stability of the self-inclusion structure $\mathbf{1}_{conf1}$? With this thought, the *N*-Boc stopper in $\mathbf{1}_{conf1}$ was replaced by other functional groups with different sizes (Scheme 1).

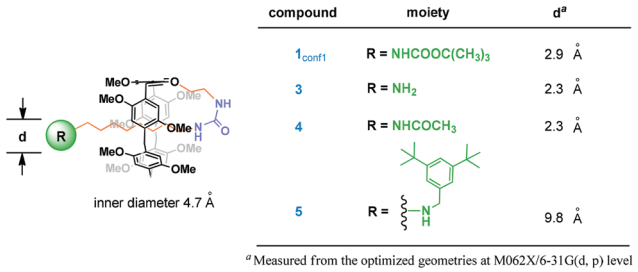

Scheme 1 Chemical structures of pseudo[1]rotaxanes with different stoppers and their calculated stopper sizes.

Firstly, deprotection of the *N*-Boc moiety of the isomer mixture of **1u**/$\mathbf{1}_{conf1}$/$\mathbf{1}_{conf2}$ in an acidic medium generated the amino-substituted compound **3**, and the self-inclusion and non-inclusion analogues of **3** cannot be separated any more due to the fast rates of the alkylamino chain's slipping in and out. Huang *et al.* have reported that an amino-modified co-pillar[5]arene with ten methylene groups tends to form cyclic dimers in $CDCl_3$ at low temperature (−35 °C).[20] But for compound **3**, in polar solvent DMSO-d_6 (Fig. 5B), the chemical shifts of the alkyl side chain protons were the same as for free 1,8-diamino octane in DMSO-d_6 (Fig. 5C), indicating that the alkyl side chain did not thread into the cavity of **P5**. However, in $CDCl_3$ the alkyl side chain protons of compound **3** shifted upfield (0.75–0 ppm) and became broad (Fig. 5A), suggesting that compound **3** existed as the self-inclusion and non-inclusion isomers with fast exchange rates on the NMR time scale in $CDCl_3$, which was also supported by the concentration-dependent ^{1}H NMR spectra of **3** in $CDCl_3$ (Fig. S5†). The self-inclusion structure of compound **3** in $CDCl_3$ could be totally destroyed in DMSO-d_6 to transform into the non-inclusion structure. When the amino group was replaced by a methyl carbonyl group, similar to **3**, the inclusion behavior of **4** is also solvent dependent (Fig. S6†): in $CDCl_3$, the protons of the alkyl chain of **4** shifted upfield and became broad, while in DMSO-d_6 the inclusion structure could not be formed.

In order to further confirm the self-inclusion structure[16,21] of compound **3** in chloroform, compound **3** was reacted with a larger stopper, 3,5-di-*tert*-butylbenzyl chloride, in chloroform to give the self-interlocked [1]rotaxane **5** in 26.6% yield, and the transformation of self-interlocked [1]rotaxane **5** into the corresponding open form was not observed. As a result, successful preparation of this self-locked [1]rotaxane **5** confirmed that compound **3** could form a relatively stable self-inclusion structure in chloroform.

Therefore, all the above results have shown that the *N*-Boc moiety is one of the key factors for the formation of the self-inclusion structure $\mathbf{1}_{conf1}$. With larger or smaller size stoppers, the dynamic transformation between the self-inclusion and non-inclusion structure could not be observed in DMSO-d_6. The size of the *tert*-butoxy carbonyl moiety (~2.9 Å) is between the amino/acetyl group (~2.3 Å) and the 3,5-di-*tert*-butylbenzyl group (~9.8 Å), which makes the axle of $\mathbf{1}_{conf1}$ possible but laborious to thread into or dethread from the **P5** cavity (internal cavity diameter 4.7 Å[22]). When the axle is encapsulated by the **P5** cavity, it will be stably trapped in the cavity under the cooperative interactions of the steric effect from the bulky *N*-Boc moiety and the other non-covalent interactions, thus the self-inclusion form $\mathbf{1}_{conf1}$ is more stable than conventional pseudo[1]rotaxanes.

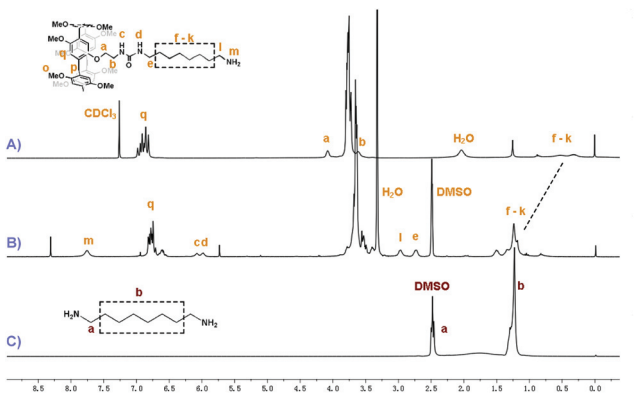

Fig. 5 ^{1}H NMR spectra (300 MHz, 298 K) of (A) **3** in $CDCl_3$, (B) **3** in DMSO-d_6, and (C) 1,8-diamino octane in DMSO-d_6.

Function of the urea moiety in the self-inclusion structure

Since the function of the *N*-Boc moiety has been revealed, we then focus on the function of the urea moiety in the self-inclusion structure $\mathbf{1}_{conf1}$. Previously, Hou *et al.*[9] reported that a pillar[5]arene bearing an amide group on the side chain could form intramolecular hydrogen bonds on the rim of **P5** and tuned the side chain into a self-inclusion conformation in the solid state. The position of the N–H bond of the amide group in **P5** is similar to the urea moiety in our case. This inspired us to further investigate the effects of the urea group of the alkyl side chain of $\mathbf{1}_{conf1}$, which might also play an important role in the formation of the self-inclusion structure by intramolecular hydrogen bonding. As discussed above, both $\mathbf{1}_{conf1}$ and $\mathbf{1}_{conf2}$ contain intramolecular H-bond between the urea moiety and the methoxy group of **P5**, therefore, with the aim of weakening the intramolecular H-bond *via* lengthening the distance between the **P5** skeleton and the urea moiety from two to four methylenes, compound **2**/**2u** was synthesized. It was found that the minor product self-inclusion form **2** and major product non-inclusion form **2u** (Scheme 2) could also

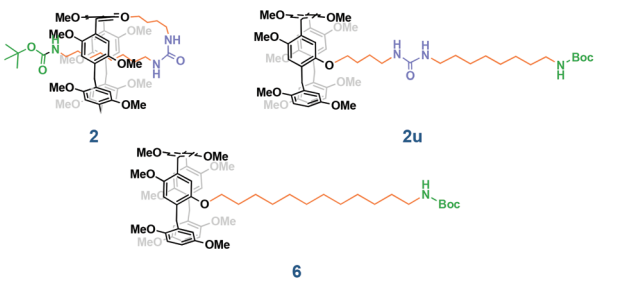

Scheme 2 Chemical structures of compounds **2**, **2u** and **6**.

be obtained and isolated *via* column chromatography in 4% and 62% yields, respectively.

Comparing the chemical shifts of the urea protons of compounds $\mathbf{1}_{conf1}$, **1u**, **2**, and **2u** (Fig. 6A–6D), it is interesting to note that the two urea peaks of the open form **1u** or **2u** are adjacent in the spectra, while the urea peaks of compound $\mathbf{1}_{conf1}$ showed a much lower shift for H_c (6.43 ppm) than H_d (5.90 ppm), indicating H_c forms intramolecular hydrogen bonds with oxygen-donor atoms in $\mathbf{1}_{conf1}$. In the spectrum of **2**, H_e (6.43 ppm) is only 0.28 ppm lower than H_f (5.89 ppm), which could be interpreted as that increasing the length between the urea moiety and the **P5** backbone weakened the intramolecular H-bonds. Based on the ^{1}H NMR spectra, the transformation between **2** and **2u** (Fig. S8†) in DMSO was much simpler compared to both $\mathbf{1}_{conf1}$ and **1u** because the third isomer could not be observed in this case. Dethreading behavior of **2** occurred at an extremely slow rate at around 20 °C in DMSO, and after 50 days the threaded methylene signals H_i could hardly be identified any more (spectrum f in Fig. S8†), suggesting that the self-inclusion structure of **2** becomes relatively unstable in polar solvent after lengthening the distance between the urea moiety and the **P5** cavity.

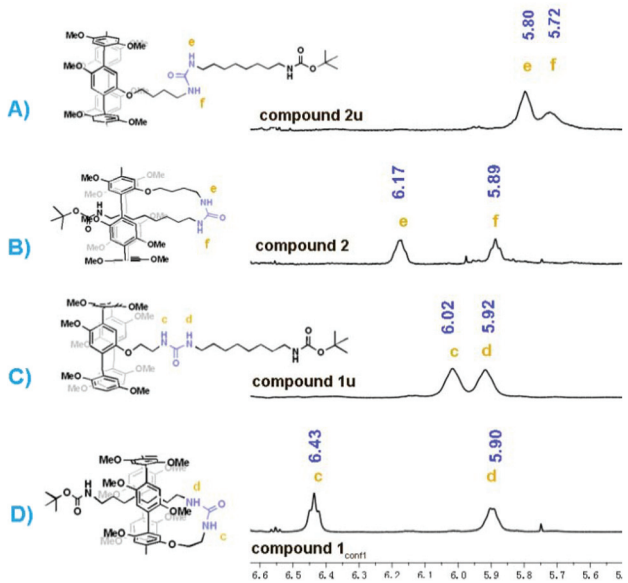

Fig. 6 The urea proton signals of (A) **2u**, (B) **2**, (C) **1u**, and (D) $\mathbf{1}_{conf1}$ in ^{1}H NMR spectra (400 MHz, DMSO-d_6, 298 K). The value of the chemical shift (ppm) is labeled above in blue.

Furthermore, another pillar[5]arene derivative **6** (Scheme 2) without the urea moiety on the alkyl side chain was synthesized and further investigated. It could form the self-inclusion structure only in $CDCl_3$ as indicated by four peaks in the upfield region from 0.5 to −2.0 ppm (Fig. 7A), while the inclusion structure was totally destroyed in DMSO-d_6 (Fig. 7B). This phenomenon also confirmed that the urea moiety plays an important role in the self-inclusion behavior of $\mathbf{1}_{conf1}$ and $\mathbf{1}_{conf2}$ by intramolecular hydrogen bonding between the urea moiety and methoxy groups of **P5**.

The formation pathway of the threaded form $\mathbf{1}_{conf1}$

We proposed three possible pathways for the formation of the pseudo[1]rotaxane product $\mathbf{1}_{conf1}$ (Fig. 8): (Path I) a Reaction-Followed-By-Threading process, which means the carbonyl imidazolium reacts with the amino group first to form the urea moiety outside the **P5** cavity, then the *N*-Boc side chain threads into the cavity and is further stabilized by the hydrogen bonding and multiple C–H···π interactions. In order for the molecule to transform slowly from **1u** to $\mathbf{1}_{conf1}$, the *tert*-butyl group must overcome the confines of the limited pillar-shaped cavity. (Path II) A Threading-Followed-By-Reaction process, which means $\mathbf{1}_{conf1}$ was produced from the *in situ* generated pseudo[2]rotaxane **8** ⊃ **9**. (Path III) Unit tumbling,[23]

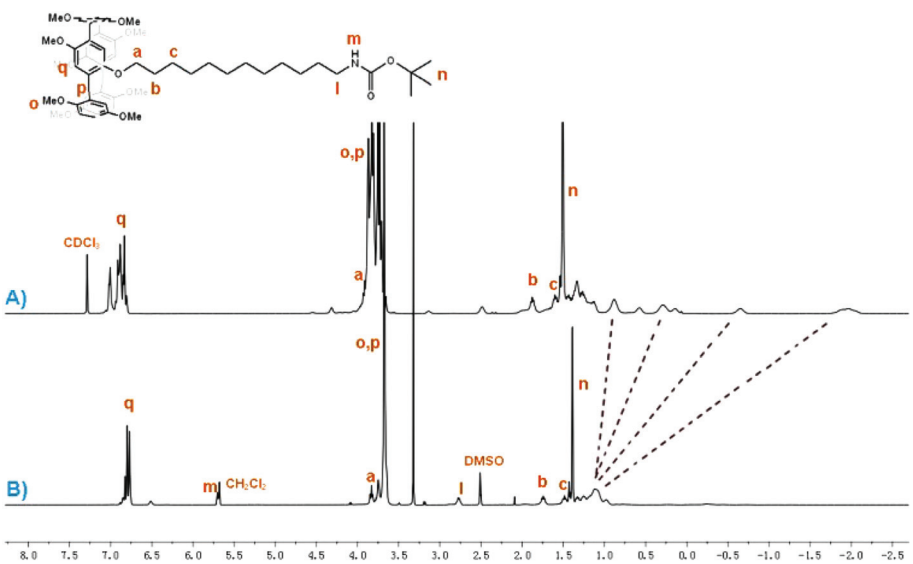

Fig. 7 ^{1}H NMR spectra of **6** in (A) $CDCl_3$ and (B) DMSO-d_6 (400 MHz, 298 K).

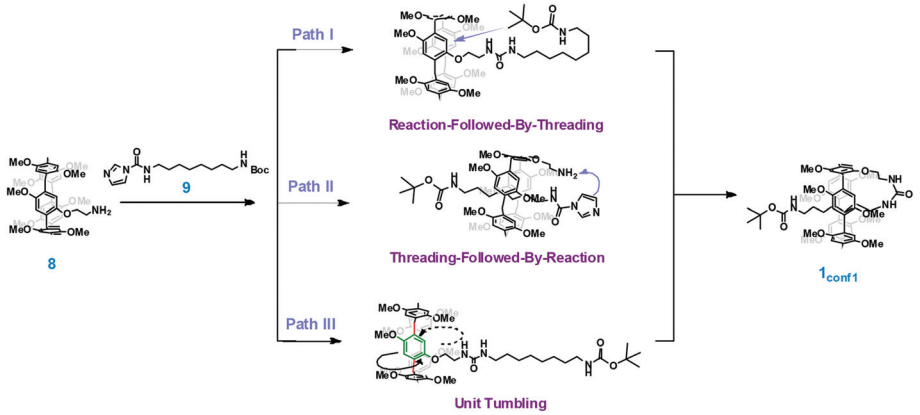

Fig. 8 Proposed pathways for the formation of pseudo[1]rotaxane.

meaning that the unthreaded **1u** is converted into pseudo[1]-rotaxane through tumbling of the hydroquinone unit.

In order to reveal the real path of our case, we designed a control experiment, in which compound **11** with the bulky triphenylchloromethyl moiety taking the place of the *N*-Boc protection moiety was reacted with compound **8** (Scheme 3). If path (II) or (III) is possible, [1]rotaxane-like compound 7 is envisioned as one of the product. However, it turned out that only the unlocked product **7u** was obtained in a yield of 44.1%, and no trace of 7 was observed. This result supported that the formation of $\mathbf{1}_{conf1}$ is a Reaction-Followed-By-Threading process.

Conclusions

In summary, we reported the preparation of an unconventional pseudo[1]rotaxane, whose threaded form $\mathbf{1}_{conf1}$ and open form **1u** could be isolated temporarily, and the self-inclusion structure of $\mathbf{1}_{conf1}$ was proved *via* HR-ESI-MS, varying concentration ^{1}H NMR, and 2D ROESY NMR measurements. Different from previously reported pseudo[1]rotaxanes, it could be clearly observed from the NMR spectra that **1u** and $\mathbf{1}_{conf1}$ both could spontaneously and slowly isomerize into mixtures of **1u**, $\mathbf{1}_{conf1}$ and the third newly appeared threaded form $\mathbf{1}_{conf2}$ in polar solvent DMSO, respectively. The conformations of **1u**, $\mathbf{1}_{conf1}$ and $\mathbf{1}_{conf2}$ were further evaluated and supported by computational calculations. In the following series of control experiments on appropriate-size stoppers, we found that the cooperative effect of the steric *N*-Boc moiety, intramolecular hydrogen bonding of the urea moiety and other non-covalent interactions were the essential factors for this special threading phenomenon in polar solvent. The discovery of this dynamic pseudo[1]rotaxane $\mathbf{1}_{conf1}$ represents a special type of inclusion phenomenon, and further studies on the controllable switch of the pseudo[1]rotaxane through anions and competitive guests are now ongoing in our lab.

Experimental

Materials and methods

All reactions were performed under the atmosphere unless noted. Commercially available reagents and solvents were employed without further purification. ^{1}H NMR spectra were recorded at 300 and 400 MHz and are reported relative to deuterated solvent signals. Data for ^{1}H NMR spectra are reported as follows: chemical shift (δ, ppm), multiplicity, coupling constant (Hz), and integration. Splitting patterns are designated as follows: s, singlet; d, doublet; t, triplet; q, quartet; m, multiplet; and br, broad. ^{13}C NMR spectra were recorded at 75 and 100 MHz. Data for ^{13}C NMR spectra are reported in terms of chemical shift. The chemical shifts are reported in parts per million (δ, ppm). The Fourier transform infrared (FTIR) samples were prepared as thin films on KBr plates, and

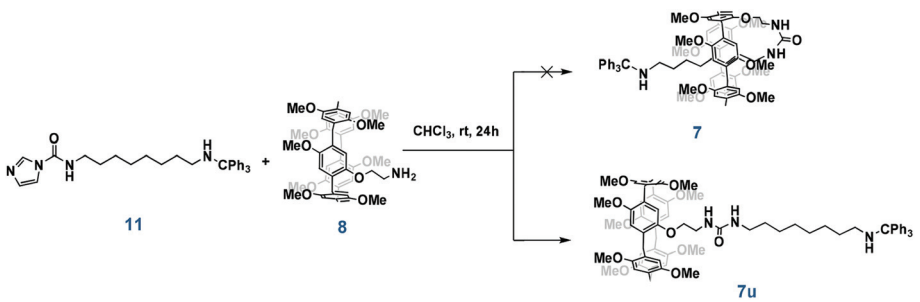

Scheme 3 Control experiment.

spectra were recorded on a spectrometer and are reported in terms of frequency of absorption (cm^{-1}). Thin-layer chromatography (TLC) was carried out using precoated silica gel sheets. Flash chromatography was performed with silica gel (200–300 mesh) with compressed air. Compounds not mentioned in the manuscript are the synthetic precursors: compound **10** is the precursor of **9**, compound **12** is the precursor of **11**, compounds **13–15** are the precursors of **2**/**2u**, compounds **16–18** are the precursors of **6**. See the ESI† for details.

Pseudo[1]rotaxane $\mathbf{1}_{conf1}$/1u. The procedure for reacting imidazolides with amine is exemplified by the synthesis of monofunctional ureidopyrimidinone.[13] Compound **9** (0.4 g, 1.18 mol) and **8** (0.858 g, 1.1 mmol) were dissolved in $CHCl_3$ (20 mL) and this solution was stirred overnight under nitrogen at 25 °C. The reaction mixture was washed with saturated $NaHCO_3$ solution (20 mL) and brine (20 mL). After drying with Na_2SO_4, the organic layer was removed by evaporation *in vacuo*. Column chromatography was used in the final separation with CH_2Cl_2–CH_3OH (140 : 1, v/v) as the eluent, to give **1u** (0.647 g, 56%) and $\mathbf{1}_{conf1}$ (0.070 g, 6%) as white solid.

$\mathbf{1}_{conf1}$: FT IR (KBr) ν (cm^{-1}) = 3417.2, 3370.6, 2933.4, 2847.2, 2834.9, 2482.1, 2147.7, 2039.6, 1713.7, 1643.3, 1561.5, 1560.1, 1497.4, 1465.9, 1397.7, 1364.9, 1214.8, 1172.4, 1048.9, 882.4, 774.8, 702.9, 647.6. ^{1}H NMR (400 MHz, DMSO-d_6, 298 K) δ (ppm) = 6.84–6.79 (m, 10H), 6.43 (s, 1H), 5.89 (s, 1H), 4.51–4.46 (d, 1H), 3.85 (s, 2H), 3.75–3.63 (m, 37H), 3.50 (t, J = 4.7 Hz, 2H), 2.81 (m, 2H), 1.48 (s, 2H), 1.40 (s, 9H), 0.85 (s, 2H), 0.16 (s, 2H), −0.44 (s, 2H), −0.91 (s, 2H), −1.32 (s, 2H), −1.65 (s, 2H). ^{13}C NMR (100 MHz, DMSO-d_6, 298 K) δ (ppm) = 158.4, 156.6, 155.5, 154.5, 149.92, 149.87, 149.7, 149.6, 149.0, 148.8, 127.5, 127.2, 127.1, 113.3, 112.8, 112.4, 95.4, 77.2, 77.1, 55.39, 55.32, 51.5, 30.6, 29.9, 29.4, 28.9, 28.7, 28.2, 28.1, 27.0, 26.2, 24.8 ppm. HR-ESI-MS: m/z calcd for $C_{60}H_{79}N_3O_{13}$ $[M]^+$ 1049.5613, found $[M + H]^+$ 1050.5686, $[M + Na]^+$ 1072.5504.

1u: mp 115–117 °C. ^{1}H NMR (400 MHz, DMSO-d_6, 298 K) δ (ppm) = 6.82–6.71 (m, 10H), 6.02 (s, 1H), 5.92 (s, 1H), 4.51–4.46 (d, 1H), 3.79 (s, 2H), 3.72–3.66 (m, 37H), 3.40 (t, J = 4.7 Hz, 2H), 3.31 (water peak), 2.97 (m, 2H), 2.86 (m, 2H), 2.49 (solvent peak), 1.36 (s, 9H), 1.21 (s, 12H). ^{13}C NMR (100 MHz, DMSO-d_6, 298 K) δ (ppm) = 158.1, 155.5, 150.0, 149.9, 149.6, 149.1, 127.8, 127.5, 127.4, 127.2, 113.6, 113.3, 77.2, 55.41, 55.36, 54.9, 54.8, 30.0, 29.4, 29.3, 29.0, 28.8, 28.2, 28.1, 26.3, 26.2, 22.8. HR-ESI-MS: m/z calcd for $C_{60}H_{79}N_3O_{13}$ $[M]^+$ 1049.5613, found $[M + H]^+$ 1050.5696, $[M + Na]^+$ 1072.5526. **1u** and $\mathbf{1}_{conf1}$ are identical in the ESI-MS spectrum.

Pseudo[1]rotaxane 2/2u. The synthesis of **2** and **2u** was the same as $\mathbf{1}_{conf1}$ and **1u**. Column chromatography (CH_2Cl_2–CH_3OH v/v = 140 : 1) gave **2** (4%) and **2u** (62%) as white solid.

2: ^{1}H NMR (400 MHz, DMSO-d_6, 298 K) δ (ppm) = 6.84–6.76 (m, 10H), 6.17 (s, 1H), 5.89 (s, 1H), 3.83 (s, 2H), 3.74–3.63 (m, 37H), 3.17 (s, 2H), 2.89 (s, 1H), 2.87 (s, 1H), 1.85 (s, 2H), 1.68 (m, 2H), 1.39 (s, 9H), 1.22–1.16 (m, 6H), 0.72 (s, 2H), 0.11 (s, 2H), −0.76 (s, 2H), −2.02 (s, 2H), −2.09 (s, 2H). ^{13}C NMR (100 MHz, DMSO-d_6, 298 K) δ (ppm) = 158.1, 155.5, 149.8, 149.2, 127.5, 127.4, 114.1, 113.2, 77.2, 55.3, 30.1, 29.4, 28.9, 28.8, 28.2, 26.4, 26.2. HR-ESI-MS: m/z calcd for $C_{62}H_{83}N_3O_{13}$ $[M]^+$ 1077.5926, found $[M + H]^+$ 1078.6008.

2u: mp 109–111 °C. ^{1}H NMR (400 MHz, DMSO-d_6, 298 K) δ (ppm) = 6.79–6.76 (m, 10H), 5.80 (s, 1H), 5.72 (s, 1H), 3.82 (s, 2H), 3.74–3.66 (m, 37H), 3.06 (s, 2H), 2.94 (s, 1H), 2.88 (s, 1H), 1.74 (s, 2H), 1.60 (s, 2H), 1.37 (s, 9H), 1.22–1.16 (m, 10H). ^{13}C NMR (100 MHz, DMSO-d_6, 298 K) δ (ppm) = 158.0, 149.8, 149.6, 127.5, 127.4, 127.2, 114.1, 113.2, 95.4, 79.2, 77.2, 71.7, 67.6, 55.3, 54.9, 50.6, 30.1, 28.8, 28.2, 28.0, 26.4. **2u** and **2** are identical in the ESI-MS spectrum.

Pseudo[1]rotaxane 3. Removal of the Boc-protecting groups with TFA was performed according to the literature method.[24] A solution of $\mathbf{1}_{conf1}$/**1u** (1.34 g, 1.27 mmol) and trifluoroacetic acid (5 mL) in dichloromethane (10 mL) was stirred for 12 h, the acid and dichloromethane were removed by evaporation *in vacuo*. The dark green oil like crude product was dissolved in dichloromethane (10 mL) again and washed with saturated $NaHCO_3$ solution (2 × 20 mL). After drying with Na_2SO_4, the solvent was removed and the residue was purified by column chromatography on silica gel (CH_2Cl_2–CH_3OH v/v = 40 : 1–1 : 1) to give **3** as a white solid (0.83 g, 68.9%). Mp 111–114 °C. ^{1}H NMR (400 MHz, DMSO-d_6, 298 K): δ (ppm) = 7.75 (s, 2H), 6.80–6.60 (m, 10H), 6.08 (s, 1H), 5.98 (s, 1H), 3.77 (m, 2H), 3.68–3.63 (m, 37H), 3.39 (m, 2H), 2.97 (s, 2H), 2.73 (s, 2H), 1.51–1.18 (m, 12H). ^{13}C NMR (100 MHz, DMSO-d_6, 298 K) δ (ppm) = 158.1, 150.0, 149.98, 149.94, 149.89, 149.85, 149.1, 127.8, 127.6, 127.50, 127.45, 127.41, 127.35, 114.4, 113.6, 113.24, 113.16, 113.08, 79.2, 68.0, 55.4, 55.3, 41.2, 32.5, 30.0, 29.1, 29.0, 28.95, 28.90, 28.84, 28.77, 28.71, 26.4, 26.1. HR-ESI-MS m/z: calcd for $C_{55}H_{71}N_3O_{11}$ $[M]^+$ 949.5089, found $[M + H]^+$ 950.5419.

Pseudo[1]rotaxane 4. A solution of **3** (0.3 g, 0.32 mmol) and triethylamine (0.04 g, 0.40 mmol) in chloroform (15 mL) was stirred for 10 min, then a solution of acetyl chloride (0.03 g, 0.4 mmol) in chloroform (5 mL) was added to the reaction solution. After 30 min, the reaction was completed, monitored by TLC. The solvent was removed *in vacuo* and the residue was purified by column chromatography on silica gel (CH_2Cl_2–CH_3OH, v/v = 30 : 1), giving **4** as a white solid (0.298 g, 95.2%). Mp 125–126 °C. ^{1}H NMR (400 MHz, DMSO-d_6, 298 K) δ (ppm) = 7.70 (s, 1H), 6.82–6.72 (m, 10H), 5.99 (s, 1H), 5.85 (s, 1H), 3.80 (t, J = 6.6 Hz, 2H), 3.68–3.64 (m, 37H), 3.40 (q, J = 6.9 Hz, 2H), 2.97–2.92 (m, 4H), 1.77 (s, 3H), 1.30–1.13 (m, 12H). ^{13}C NMR (100 MHz, DMSO-d_6, 298 K) δ (ppm) = 168.8, 158.1, 149.98, 149.94, 149.91, 149.8, 149.3, 149.1, 127.7, 127.6, 127.5, 127.46, 127.40, 127.35, 114.3, 113.6, 113.3, 95.4, 68.0, 55.4, 55.34, 55.30, 29.9, 29.1, 28.9, 28.8, 26.4, 26.3, 22.6. HR-ESI-MS: m/z calcd for $C_{57}H_{73}N_3O_{12}$ $[M]^+$ 991.5194, found $[M + H]^+$ 992.5349, $[M + Na]^+$ 1014.5107.

[1]Rotaxane 5. The capping reaction was performed according to the literature method.[17] A solution of **3** (0.2 g, 0.21 mmol) and 3,5-di-*tert*-butylbenzaldehyde (0.05 g, 0.23 mmol) in chloroform (20 mL) was stirred for 24 h, then $NaBH_4$ (0.03 g, 0.8 mmol) and ethanol (5 mL) were added in the reaction solution. After another 24 h, the reaction was completed, monitored by TLC. The solvent was removed *in vacuo*

and the residue was purified by column chromatography on silica gel (CH_2Cl_2–CH_3OH, v/v = 10 : 1–6 : 1), giving **5** as a white solid (0.065 g, 26.6%). Mp 93–96 °C. ^{1}H NMR (400 MHz, DMSO-d_6, 298 K) δ (ppm) = 7.48 (s, 1H), 7.43 (s, 1H), 7.39 (s, 1H), 6.83–6.77 (m, 10H), 6.12 (s, 1H), 6.02 (s, 1H), 4.03 (s, 2H), 3.78–3.63 (m, 39H), 3.40 (m, 2H), 2.99 (m, 2H), 2.83 (m, 2H), 1.63 (m, 2H), 1.35 (s, 9H), 1.33 (s, 9H), 1.24 (m, 2H), −0.25 (br, 2H), −1.14 (br, 2H), −1.69 (br, 2H), −2.06 (br, 2H). ^{13}C NMR (100 MHz, DMSO-d_6, 298 K) δ (ppm) = 158.4, 158.3, 158.1, 150.6, 150.0, 149.8, 149.7, 149.6, 149.1, 149.0, 127.7, 127.6, 127.4, 127.2, 123.9, 122.0, 114.3, 113.7, 113.3, 112.5, 95.4, 67.9, 55.4, 55.3, 55.2, 55.1, 54.7, 52.0, 50.8, 46.8, 34.59, 34.56, 34.44, 34.34, 31.23, 31.17, 30.0, 29.1, 29.0, 28.7, 28.5, 26.9, 26.3, 26.0, 25.5. HR-ESI-MS *m*/*z*: calcd for $C_{70}H_{93}N_3O_{11}$ $[M]^+$ 1151.6810, found $[M + H]^+$ 1152.6902.

Pseudo[1]rotaxane 6. The synthesis of **6** was similar to that of **10** (see below). Yield: 45%. Mp 103–105 °C. ^{1}H NMR (400 MHz, $CDCl_3$, 298 K) δ (ppm) = 7.02–6.80 (m, 10H), 3.95–3.66 (m, 39H), 1.88 (m, 2H), 1.60 (m, 2H), 1.51 (s, 9H), 1.43 (m, 2H), 1.33 (m, 2H), 1.27 (m, 2H), 1.12 (m, 2H), 0.88 (s, 2H), 0.29 (m, 2H), −0.65 (s, 2H), −1.92 (s, 2H), −1.96 (s, 2H). ^{13}C NMR (100 MHz, $CDCl_3$, 298 K) δ (ppm) = 155.6, 154.8, 150.94, 150.90, 150.86, 150.76, 150.68, 150.5, 150.3, 150.2, 150.1, 149.8, 128.6, 128.39, 128.35, 128.24, 128.16, 128.1, 115.2, 114.3, 114.2, 113.9, 113.7, 113.1, 78.5, 68.7, 68.6, 68.4, 55.89, 55.85, 55.78, 55.72, 55.61, 55.58, 55.50, 55.3, 55.2, 40.7, 30.1, 30.0, 29.73, 29.68, 29.5, 29.4, 29.3, 29.1, 28.6, 28.5, 26.1. ^{1}H NMR (400 MHz, DMSO-d_6, 298 K) δ (ppm) = 6.79–6.75 (m, 10H), 5.69 (s, 1H), 3.82 (t, J = 6.2 Hz, 2H), 3.73–3.31 (m, 37H), 2.76 (q, J = 6.3 Hz, 2H), 1.73 (m, 2H), 1.47 (m, 2H), 1.37 (s, 9H), 1.32 (m, 2H), 1.24 (m, 2H), 1.16–0.97 (m, 10H, overlapped). ^{13}C NMR (100 MHz, DMSO-d_6, 298 K) δ (ppm) = 155.4, 149.97, 149.91, 149.87, 149.82, 149.80, 149.2, 127.49, 127.46, 127.41, 127.36, 114.1, 113.3, 113.2, 95.4, 79.2, 77.2, 67.7, 55.34, 55.27, 55.2, 54.8, 29.2, 28.9, 28.84, 28.75, 28.69, 28.61, 28.5, 28.22, 28.16, 26.2, 25.4. HR-ESI-MS: *m*/*z* calcd for $C_{61}H_{81}NO_{12}$ $[M]^+$ 1019.5759, found $[M + H]^+$ 1020.5834.

Copillar[5]arene 7u. The synthetic procedure of **7u** is similar to that of compound $\mathbf{1}_{conf1}$. Yield: 44.1%. Mp 93–96 °C. ^{1}H NMR (400 MHz, DMSO-d_6, 298 K) δ (ppm) = 7.39 (d, J = 7.6 Hz, 6H), 7.27 (t, J = 7.4 Hz, 6H), 7.15 (t, J = 7.2 Hz, 3H), 6.82–6.76 (m, 10H), 6.02 (s, 1H), 5.92 (s, 1H), 3.79 (t, 2H), 3.68–3.60 (m, 37H), 3.40 (q, 2H), 2.98 (m, 2H), 1.95 (m, 2H), 1.43 (s, 2H), 1.33 (s, 2H), 1.19 (s, 8H). ^{13}C NMR (75 MHz, DMSO-d_6, 298 K) δ (ppm) = 158.0, 150.0, 149.1, 146.3, 128.3, 127.7, 127.6, 125.9, 113.6, 113.3, 95.4, 70.4, 67.9, 55.4, 43.3, 30.0, 29.0, 28.8, 26.9, 26.4. HR-ESI-MS *m*/*z*: calcd for $C_{74}H_{85}N_3O_{11}$ $[M]^+$ 1191.6184, found $[M + H]^+$ 1192.6503, $[M + Na]^+$ 1214.6072.

***N*-(*tert*-Butoxycarbonyl)-*N*′-(imidazolylcarbonyl)-1,8-octanediamine (9).** The synthesis of **9** was according to the literature method.[13] **10** (0.67 g, 2.74 mmol) and 1,1-carbonyldiimidazole (CDI) (1.38 g, 8.5 mmol) were suspended in $CHCl_3$ (50 mL) and stirred for 12 h at room temperature. The reaction mixture was washed with saturated $NaHCO_3$ solution (40 mL) and brine (40 mL). After drying with Na_2SO_4, the organic layer was removed by evaporation *in vacuo* and the product was obtained as a buff powder (0.91 g, 98%). Remark: this compound is unstable under acidic conditions, thus **9** was utilized without further purification by silica column chromatography, which caused a little impurity in the spectrum. Mp 58–62 °C. ^{1}H NMR (300 MHz, $CDCl_3$, 298 K) δ (ppm) = 8.27 (s, 1H), 8.07 (s, 1H), 7.60 (s, 1H), 7.32 (chloroform solvent), 7.01 (s, 1H), 4.90 (s, 1H), 3.37 (q, J = 4.7 Hz, 2H), 3.06 (q, J = 5.1 Hz, 2H), 1.59 (m, 2H), 1.43 (s, 10H), 1.25 (s, 9H). ^{13}C NMR (100 MHz, $CDCl_3$, 298 K) δ (ppm) = 156.3, 149.2, 136.1, 129.5, 116.5, 79.1, 57.9, 40.9, 40.5, 30.0, 29.2, 28.9, 28.4, 26.6, 26.5. HR-ESI-MS: *m*/*z* calcd for $C_{17}H_{30}N_4O_3$ $[M]^+$, 338.2318, found $[M + H]^+$ 339.2521, $[M + Na]^+$ 361.2215.

***N*-(*tert*-Butoxycarbonyl)-1,8-octanediamine (10).** Mono-protection of diamines with the Boc group was performed according to the literature method.[24] A solution of Boc_2O (2.42 g, 12 mmol) in $CHCl_3$ (40 mL) was added dropwise over a 2 h period to the solution of 1,8-diamino octane (3.46 g, 24 mmol) and TEA (2.42 g, 24 mmol) in $CHCl_3$ (150 mL) cooled with an ice-bath. The reaction mixture was stirred overnight at room temperature and filtered. The filtrate was concentrated under vacuum and the resulting oil dissolved in $CHCl_3$ (100 mL) was washed with H_2O (6 × 100 mL) until 1,8-diamino octane could not be observed by TLC, the organic layer was dried with anhydrous $MgSO_4$ and concentrated under vacuum to afford pure mono-Boc-protected diamine **10**. Further purification by silica column chromatography (CH_2Cl_2–CH_3OH, v/v = 200 : 1–60 : 1) gave **10** as a white solid (1.30 g, 36.5%). Mp 73–74 °C. ^{1}H NMR (300 MHz, $CDCl_3$, 298 K) δ (ppm) = 4.56 (s, 1H), 3.08 (q, J = 6.5 Hz, 2H), 2.66 (t, J = 7.0 Hz, 2H), 1.65 (s, 2H), 1.42 (s, 12H), 1.28 (s, 9H). ^{13}C NMR (100 MHz, $CDCl_3$, 298 K) δ (ppm) = 163.5, 156.0, 78.8, 41.7, 41.3, 40.5, 32.2, 30.6, 30.0, 29.2, 29.1, 28.4, 26.7. HR-ESI-MS: *m*/*z* calcd for $C_{13}H_{28}N_2O_2$ $[M]^+$ 244.2151, found $[M + H]^+$ 245.2290, $[M + Na]^+$ 267.2044.

***N*-(Triphenylmethyl)-*N*′-(imidazolylcarbonyl)-1,8-octanediamine (11).** Compound **11** was synthesized in a similar way as that of **9**. Yield: 99%. Mp 93–96 °C. ^{1}H NMR (300 MHz, $CDCl_3$, 298 K) δ (ppm) = 8.17 (s, 1H), 7.46 (d, J = 7.3 Hz, 6H), 7.40 (s, 1H), 7.26 (chloroform solvent), 7.25 (t, J = 6.2 Hz, 6H), 7.16 (t, J = 7.2 Hz, 3H), 7.01 (s, 1H), 3.37 (q, J = 6.4 Hz, 2H), 2.11 (t, J = 7.0 Hz, 2H), 1.61–1.26 (m, 12H). ^{13}C NMR (100 MHz, $CDCl_3$, 298 K) δ (ppm) = 149.0, 146.3, 135.8, 130.0, 128.7, 127.8, 126.2, 116.3, 96.1, 71.0, 64.5, 43.6, 41.1, 30.8, 29.5, 29.2, 27.3, 26.8, 14.2. HR-ESI-MS *m*/*z*: calcd for $C_{32}H_{37}N_3O$ $[M]^+$ 479.2937, found $[M + H]^+$ 481.2978, $[M + Na]^+$ 503.2784.

***N*-(Triphenylmethyl)-1,8-octanediamine (12).** Compound **12** was synthesized in a similar way as that of **10**, colorless oil, yield: 36.5%. ^{1}H NMR (300 MHz, $CDCl_3$, 298 K) δ (ppm) = 7.49 (d, J = 7.4 Hz, 6H), 7.28 (t, J = 7.1 Hz, 6H), 7.18 (t, J = 7.1 Hz, 3H), 2.68 (t, J = 6.9 Hz, 2H), 2.12 (t, J = 6.9 Hz, 2H), 1.48–1.27 (m, 16H). ^{13}C NMR (100 MHz, $CDCl_3$, 298 K) δ (ppm) = 146.4, 128.7, 127.8, 126.2, 70.9, 43.6, 42.3, 33.9, 30.9, 29.7, 29.5, 27.4, 26.9. HR-ESI-MS *m*/*z*: calcd for $C_{27}H_{34}N_2$ $[M]^+$ 386.2722, found $[M + H]^+$ 387.2795.

1-(4-Bromo-*n*-butoxy)-4-methoxybenzene (13). The synthetic procedure of **13** is according to the literature,[25] yield 85.9%.

Mp 31–32 °C. ^{1}H NMR (400 MHz, $CDCl_3$, 298 K) δ (ppm) = 6.80 (s, 4H), 3.90 (t, J = 4 Hz, 2H), 3.73 (s, 3H), 3.45 (t, J = 5 Hz, 2H), 2.04–2.01 (m, 2H), 1.90–1.86 (m, 2H). ^{13}C NMR (100 MHz, $CDCl_3$, 298 K) δ (ppm) = 153.9, 153.1, 115.5, 114.7, 67.5, 55.7, 33.6, 29.6, 28.1 ppm. LR-ESI-MS m/z: calcd for $C_{11}H_{15}BrO_2$ $[M]^+$ 258.0255, found $[M + H]^+$ 259.00, $[M + K]^+$ 296.10.

Copillar[5]arene 14. **14** was synthesized according to a reported method.[26] Paraformaldehyde (1.80 g, 60.0 mmol) was added to a solution of 1,4-dimethoxybenzene (2.75 g, 20.0 mmol) and 1-(4-bromobutoxy)-4-methoxybenzene (0.32 g, 1.25 mmol) in dry CH_2Cl_2 (150 mL) under a nitrogen atmosphere. Anhydrous $FeCl_3$ (0.52 g, 3.2 mmol) was then added to the solution and the mixture was stirred in an ice bath for 2.5 h. The solution was then washed with H_2O (150 mL). The organic layer was dried with anhydrous Na_2SO_4, concentrated under vacuum, and subjected to silica column chromatography (hexanes–CH_2Cl_2 v/v = 1 : 3) to give **14** (0.11 g, 10%). Mp 99–102 °C. ^{1}H NMR (400 MHz, DMSO-d_6, 298 K) δ (ppm) = 6.85–6.75 (m, 10H, Ar*H*), 3.86 (t, J = 6.1 Hz, 2H), 3.81–3.61 (m, 37H), 3.50 (t, J = 6.4 Hz, 2H), 1.92 (m, 2H), 1.81 (m, 2H). ^{13}C NMR (75 MHz, DMSO-d_6, 298 K) δ (ppm) = 153.3, 153.0, 151.2, 150.0, 149.2, 129.3, 127.5, 116.4, 114.6, 114.2, 113.2, 111.4, 110.9, 95.4, 67.1, 55.7, 55.4, 34.5, 29.5, 28.9, 27.9. HR-ESI-MS m/z: calcd for $C_{48}H_{55}BrO_{10}$ $[M]^+$ 870.2979, found $[M + NH_4]^+$ 888.3342.

Copillar[5]arene 15. The synthetic procedure of **15** is similar to our previous work,[27] the combined yield from **13** to **15** is calculated to be 20.0%. Mp 113–116 °C. ^{1}H NMR (400 MHz, DMSO-d_6, 298 K) δ (ppm) = 6.79–6.76 (m, 10H), 3.81 (t, 2H, J = 6.3 Hz), 3.65 (m, 37H), 2.57 (t, J = 6.8 Hz, 2H), 1.73 (m, 2H), 1.52 (m, 2H). ^{13}C NMR (100 MHz, DMSO-d_6, 298 K) δ (ppm) = 149.9, 127.5, 114.0, 113.3, 95.4, 67.7, 55.4, 28.9, 26.6. HR-ESI-MS m/z: calcd for $C_{48}H_{57}NO_{10}$ $[M]^+$ 807.3982, found $[M + H]^+$ 808.4321, $[M + Na]^+$ 830.3894.

1-(12-Bromododecyl)-4-methoxybenzene (16). The synthetic procedure of **16** is similar to that of compound **13**. Yield: 81.75%. Mp 38–42 °C. ^{1}H NMR (300 MHz, $CDCl_3$, 298 K) δ (ppm) = 7.26 (solvent peak), 6.83 (s, 4H, Ar*H*), 3.90 (t, J = 5.0 Hz, 2H), 3.76 (s, 3H), 3.40 (t, J = 5.2 Hz, 2H), 1.85 (m, 2H), 1.75 (m, 2H), 1.43–1.26 (m, 16H). ^{13}C NMR (75 MHz, $CDCl_3$, 298 K) δ (ppm) = 153.7, 153.3, 115.4, 114.6, 55.7, 34.0, 32.9, 29.6, 29.5, 29.4, 28.8, 28.2, 26.1. HR-ESI-MS: m/z calcd for $C_{19}H_{31}BrO_2$ $[M]^+$, 370.1507, found $[M + H]^+$ 371.1581.

Copillar[5]arene 17. The synthetic procedure of **17** is similar to that of compound **14**. Mp 178–180 °C. ^{1}H NMR (400 MHz, DMSO-d_6, 298 K) δ (ppm) = 6.85–6.75 (m, 10H, Ar*H*), 3.84 (t, J = 6.1 Hz, 2H), 3.77–3.63 (m, 37H), 3.50 (t, J = 6.4 Hz, 2H), 1.92 (m, 2H), 1.81 (m, 2H). ^{13}C NMR (100 MHz, $CDCl_3$, 298 K) δ (ppm) = 150.5, 150.4, 150.3, 150.2, 149.8, 128.0, 113.7, 113.3, 113.2, 113.0, 68.5, 55.6, 55.4, 55.3, 33.7, 31.6, 30.0, 29.3, 29.2, 28.2, 27.7, 25.6. HR-ESI-MS m/z: calcd for $C_{56}H_{71}BrO_{10}$ $[M]^+$ 982.4231, found $[M + NH_4]^+$ 1000.4586.

Copillar[5]arene 18. The synthetic procedure of **18** is similar to that of compound **15**, the combined yield from **16** to **18** is calculated to be 24.6%. Mp 112–114 °C. ^{1}H NMR (400 MHz, DMSO-d_6, 298 K) δ (ppm) = 6.79–6.75 (m, 10H), 3.80 (m, 2H), 3.66–3.64 (m, 37H), 2.08 (t, J = 5 Hz, 2H), 1.71 (m, 2H), 1.41 (m, 2H), 1.1 (m, 2H), 1.11–0.82 (m, 10H), 0.68 (s, 4H). ^{13}C NMR (100 MHz, DMSO-d_6, 298 K) δ (ppm) = 149.8, 127.4, 112.9, 95.5, 67.7, 55.0, 41.2, 32.5, 29.4, 29.3, 29.2, 29.1, 25.8. HR-ESI-MS m/z: calcd for $C_{56}H_{73}NO_{10}$ $[M]^+$ 919.5234, found $[M + H]^+$ 920.5329, $[M + Na]^+$ 942.4845.

Acknowledgements

We gratefully thank the National Basic Research Program of China (2011CB808600) and the National Natural Science Foundation of China (nos. 20932004, 21072093, 21202083, 91227106) for financial support.

Notes and references

1 (*a*) D. B. Amabilino and J. F. Stoddart, *Chem. Rev.*, 1995, **95**, 2725–2828; (*b*) F. M. Raymo and J. F. Stoddart, *Chem. Rev.*, 1999, **99**, 1643–1664; (*c*) X. Ma and H. Tian, *Chem. Soc. Rev.*, 2010, **39**, 70–80; (*d*) R. S. Forgan, J.-P. Sauvage and J. F. Stoddart, *Chem. Rev.*, 2011, **111**, 5434–5464; (*e*) J. Rotzler and M. Mayor, *Chem. Soc. Rev.*, 2013, **42**, 44–62.

2 (*a*) Y. Han, K. Cheng, K. A. Simon, Y. Lan, P. Sejwal and Y.-Y. Luk, *J. Am. Chem. Soc.*, 2006, **128**, 13913–13920; (*b*) C. Binkowski, F. Hapiot, V. Lequart, P. Martin and E. Monflier, *Org. Biomol. Chem.*, 2005, **3**, 1129–1133; (*c*) K. K. Park, Y. S. Kim, S. Y. Lee, H. E. Song and J. W. Park, *J. Chem. Soc., Perkin Trans. 2*, 2001, 2114–2118; (*d*) K. Yamauchi, A. Miyawaki, Y. Takashima, H. Yamaguchi and A. Harada, *Org. Lett.*, 2010, **12**, 1284–1286.

3 (*a*) P. R. Ashton, R. Ballardini, V. Balzani, S. E. Boyd, A. Credi, M. T. Gandolfi, M. Gómez-López, S. Iqbal, D. Philp, J. A. Preece, L. Prodi, H. G. Ricketts, J. F. Stoddart, M. S. Tolley, M. Venturi, A. J. P. White and D. J. Williams, *Chem.–Eur. J.*, 1997, **3**, 152–170; (*b*) R. Corradini, A. Dossena, R. Marchelli, A. Panagia, G. Sartor, M. Saviano, A. Lombardi and V. Pavone, *Chem.–Eur. J.*, 1996, **2**, 373–381; (*c*) Y. Liu, Z.-X. Yang and Y. Chen, *J. Org. Chem.*, 2008, **73**, 5298–5304.

4 (*a*) X. Ma, D. Qu, F. Ji, Q. Wang, L. Zhu, Y. Xu and H. Tian, *Chem. Commun.*, 2007, 1409–1411; (*b*) K. Hiratani, M. Kaneyama, Y. Nagawa, E. Koyama and M. Kanesato, *J. Am. Chem. Soc.*, 2004, **126**, 13568–13569.

5 (*a*) Y. Inoue, P. Kuad, Y. Okumura, Y. Takashima, H. Yamaguchi and A. Harada, *J. Am. Chem. Soc.*, 2007, **129**, 6396–6397; (*b*) H. Ikeda, M. Nakamura, N. Ise, N. Oguma, A. Nakamura, T. Ikeda, F. Toda and A. Ueno, *J. Am. Chem. Soc.*, 1996, **118**, 10980–10988; (*c*) H. F. M. Nelissen, F. Venema, R. M. Uittenbogaard, M. C. Feiters and R. J. M. Nolte, *J. Chem. Soc., Perkin Trans. 2*, 1997, 2045–2053; (*d*) A. Ueno, A. Ikeda, H. Ikeda, T. Ikeda and F. Toda, *J. Org. Chem.*, 1999, **64**, 382–387; (*e*) V. Balzani, P. Ceroni, A. Credi, M. Gomez-Lopez, C. Hamers, J. F. Stoddart and

R. Wolf, *New J. Chem.*, 2001, **25**, 25–31; (*f*) S. Nygaard, Y. Liu, P. C. Stein, A. H. Flood and J. O. Jeppesen, *Adv. Funct. Mater.*, 2007, **17**, 751–762; (*g*) H. Li, H. Zhang, Q. Zhang, Q.-W. Zhang and D.-H. Qu, *Org. Lett.*, 2012, **14**, 5900–5903; (*h*) C. Clavel, C. Romuald, E. Brabet and F. Coutrot, *Chem.–Eur. J.*, 2013, **19**, 2982–2989; (*i*) T. Ogoshi, R. Shiga and T. A. Yamagishi, *J. Am. Chem. Soc.*, 2012, **134**, 4577–4580; (*j*) T. Ogoshi, N. Ueshima, T.-A. Yamagishi, Y. Toyota and N. Matsumi, *Chem. Commun.*, 2012, **48**, 3536–3538.

6 (*a*) T. Ogoshi, S. Kanai, S. Fujinami, T. A. Yamagishi and Y. Nakamoto, *J. Am. Chem. Soc.*, 2008, **130**, 5022–5023; (*b*) D. Cao, Y. Kou, J. Liang, Z. Chen, L. Wang and H. Meier, *Angew. Chem., Int. Ed.*, 2009, **48**, 9721–9723.

7 (*a*) C. Li, Q. Xu, J. Li, F. Yao and X. Jia, *Org. Biomol. Chem.*, 2010, **8**, 1568–1576; (*b*) C. Li, L. Zhao, J. Li, X. Ding, S. Chen, Q. Zhang, Y. Yu and X. Jia, *Chem. Commun.*, 2010, **46**, 9016–9018; (*c*) C. Li, X. Shu, J. Li, J. Fan, Z. Chen, L. Weng and X. Jia, *Org. Lett.*, 2012, **14**, 4126–4129; (*d*) L. Gao, C. Han, B. Zheng, S. Dong and F. Huang, *Chem. Commun.*, 2013, **49**, 472–474; (*e*) X.-B. Hu, L. Chen, W. Si, Y. Yu and J.-L. Hou, *Chem. Commun.*, 2011, **47**, 4694–4696.

8 Y. Chen, D. Cao, L. Wang, M. He, L. Zhou, D. Schollmeyer and H. Meier, *Chem.–Eur. J.*, 2013, **19**, 7064–7070.

9 L. Chen, Z. Li, Z. Chen and J.-L. Hou, *Org. Biomol. Chem.*, 2013, **11**, 248–251.

10 T. Ogoshi, K. Demachi, K. Kitajima and T. A. Yamagishi, *Chem. Commun.*, 2011, **47**, 7164–7166.

11 Q. Duan, W. Xia, X. Hu, M. Ni, J. Jiang, C. Lin, Y. Pan and L. Wang, *Chem. Commun.*, 2012, **48**, 8532–8534.

12 M. Ni, Y. Guan, L. Wu, C. Deng, X. Hu, J. Jiang, C. Lin and L. Wang, *Tetrahedron Lett.*, 2012, **53**, 6409–6413.

13 P. Y. W. Dankers, P. J. H. M. Adams, D. W. P. M. Löwik, J. C. M. van Hest and E. W. Meijer, *Eur. J. Org. Chem.*, 2007, 3622–3632.

14 (*a*) M. Boiocchi, L. Del Boca, D. E. Gómez, L. Fabbrizzi, M. Licchelli and E. Monzani, *J. Am. Chem. Soc.*, 2004, **126**, 16507–16514; (*b*) C. Perez-Casas and A. K. Yatsimirsky, *J. Org. Chem.*, 2008, **73**, 2275–2284; (*c*) V. Amendola, L. Fabbrizzi and L. Mosca, *Chem. Soc. Rev.*, 2010, **39**, 3889–3915.

15 L. Liu, Y. Liu, P. Liu, J. Wu, Y. Guan, X. Hu, C. Lin, Y. Yang, X. Sun, J. Ma and L. Wang, *Chem. Sci.*, 2013, **4**, 1701–1706.

16 T. Ogoshi, Y. Nishida, T. A. Yamagishi and Y. Nakamoto, *Macromolecules*, 2010, **43**, 7068–7072.

17 N. L. Strutt, R. S. Forgan, J. M. Spruell, Y. Y. Botros and J. F. Stoddart, *J. Am. Chem. Soc.*, 2011, **133**, 5668–5671.

18 P. Wei, X. Yan, J. Li, Y. Ma, Y. Yao and F. Huang, *Tetrahedron*, 2012, **68**, 9179–9185.

19 X.-Y. Hu, X. Wu, Q. Duan, T. Xiao, C. Lin and L. Wang, *Org. Lett.*, 2012, **14**, 4826–4829.

20 Z. Zhang, C. Han, G. Yu and F. Huang, *Chem. Sci.*, 2012, **3**, 3026–3031.

21 T. Ogoshi, Y. Hasegawa, T. Aoki, Y. Ishimori, S. Inagi and T.-A. Yamagishi, *Macromolecules*, 2011, **44**, 7639–7644.

22 M. Xue, Y. Yang, X. Chi, Z. Zhang and F. Huang, *Acc. Chem. Res.*, 2012, **45**, 1294–1308.

23 T. Ogoshi, T. Akutsu, D. Yamafuji, T. Aoki and T.-A. Yamagishi, *Angew. Chem., Int. Ed.*, 2013, **52**, 8111–8115.

24 C. Dardonville, C. Fernandez-Fernandez, S.-L. Gibbons, G. J. Ryan, N. Jagerovic, A. M. Gabilondo, J. J. Meana and L. F. Callado, *Bioorg. Med. Chem.*, 2006, **14**, 6570–6580.

25 D. M. Schultz, J. A. Prescher, S. Kidd, D. Marona-Lewicka, D. E. Nichols and A. Monte, *Bioorg. Med. Chem.*, 2008, **16**, 6242–6251.

26 L. Liu, D. Cao, Y. Jin, H. Tao, Y. Kou and H. Meier, *Org. Biomol. Chem.*, 2011, **9**, 7007–7010.

27 Y. Guan, M. Ni, X. Hu, T. Xiao, S. Xiong, C. Lin and L. Wang, *Chem. Commun.*, 2012, **48**, 8529–8531.